Identification of an elasto-viscoplasticity damage model for a copper alloy submitted to extreme thermo-mechanical loading

S. VINCENT[a], R. BILLARDON[a].

a. LMT-Cachan (ENS Cachan / CNRS (UMR 8535) / UPMC Univ. Paris 06)
61, av. du Président Wilson, F-94235 Cachan Cedex, France. +33147402193, name(at)lmt.ens-cachan.fr

Résumé :

La chambre de combustion d'un moteur fusée subit des chargements thermomécaniques monotones et cycliques complexes sur des plages de vitesses de déformations et de températures respectivement comprises entre [10^{-6} s^{-1}, 10^{-1} s^{-1}] et [0.015 T_m, 0.80 T_m] où T_m représente la température de fusion du matériau.

L'alliage de cuivre considéré ici est durci par précipitation. L'accent est mis sur la procédure d'identification et la robustesse d'un modèle de type Chaboche à plusieurs écrouissages et mécanismes d'endommagement.

Abstract:

In service, liquid rocket engine chambers are submitted to monotonic and cyclic thermo-mechanical loading within the strain rate range [10^{-6} s^{-1}, 10^{-1} s^{-1}] and the temperature range [0.015 T_m, 0.80 T_m] where T_m denotes the melting temperature of the material.

The copper alloy considered herein is hardened by precipitation. Emphasis is put on the identification procedure and the robustness of a Chaboche type model with different hardening and damage mechanisms.

Mots clefs : copper alloy, elasto-viscoplasticity, damage, extreme loading, identification, robustness.

1 Introduction

Lifetime of Liquid Rocket Engine chambers is one of the major issues for the feasibility of next generation of launchers and in particular for reusable launch systems. Because of the complexity of the thermomecanical loading imposed on the chamber materials, the prediction of this lifetime requires efficient tools and especially the identification of robust behaviour models over a large amplitude validity range (see Figure 1).

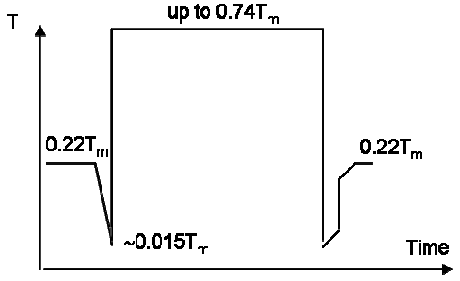

FIG. 1: Typical evolution of the temperature in the wall of a combustion chamber for a start-stop cycle

In that context, and after several mechanical studies previously made using Elasto-ViscoPlastic (EVP)

constitutive equations, Snecma in collaboration with LMT-Cachan managed to identify and implement into a finite element software a coupled Elasto-ViscoPlasticity Damage (D-EVP) model.

Before the development of this model, the complete structural analysis was performed with a similar Elasto-ViscoPlastic (EVP) model and damage evolution in critical points of the structure was subsequently evaluated using a linear accumulation law. The main advantage of the coupled approach is to take account of the influence of the damage evolution while predicting the mechanical behaviour of the material all along the operating phases of the engine.

2 An elasto-viscoplasticity damage model

This hierarchic model belongs to the class of elasto-viscoplastic models coupled to continuum damage models [1]. The hypothesis of a state decoupling between hardening and elasticity on one hand, and between hardening and damage on the other hand, is made.

Small strain assumption and standard strain partition are made so that

$$\underline{\underline{\varepsilon}} = \underline{\underline{\varepsilon}}^{e} + \underline{\underline{\varepsilon}}^{p} \tag{1}$$

where $\underline{\underline{\varepsilon}}$, $\underline{\underline{\varepsilon}}^{e}$ and $\underline{\underline{\varepsilon}}^{p}$ respectively denote the total, elastic, and (visco)plastic strain tensors.

The thermo-elastic law is written as

$$\underline{\underline{\varepsilon}}^{e} = \frac{1}{(1-D_d)(1-D_c)} \underline{\underline{\underline{E}}}_{(T)}^{-1} : \underline{\underline{\sigma}} + \alpha_{(T;T_{ref})} \left(T - T_{ref}\right) \underline{\underline{I}} \tag{2}$$

where $\underline{\underline{\sigma}}$ denotes the stress tensor, T the temperature, D_c and D_d two scalar damage variables, and where $\underline{\underline{\underline{E}}}_{(T)}$ and $\alpha_{(T\,;\,Tref)}$ are the standard elasticity tensor and linear thermal expansion scalar coefficient.

The elastic domain is written as

$$f_p = \frac{J_2\left(\underline{\underline{\sigma}} - \underline{\underline{X}}_1 - \underline{\underline{X}}_2\right)}{\left(1-D_d\right)\left(1-D_c\right)} - \left(R_1 + R_2\right) - \sigma_{y_{(T)}} \tag{3a}$$

$$\text{with} \quad J_2\left(\underline{\underline{\sigma}} - \underline{\underline{X}}_1 - \underline{\underline{X}}_2\right) = \sqrt{\frac{3}{2}\left(\underline{\underline{\sigma}}^{D} - \underline{\underline{X}}_1 - \underline{\underline{X}}_2\right) : \left(\underline{\underline{\sigma}}^{D} - \underline{\underline{X}}_1 - \underline{\underline{X}}_2\right)} \tag{3b}$$

where $\underline{\underline{\sigma}}^{D}$ denotes the deviatoric stress tensor, $\underline{\underline{X}}_1$ and $\underline{\underline{X}}_2$ two kinematic hardening variables, R_1 and R_2 two isotropic hardening variables, and where $\sigma_{y_{(T)}}$ is the initial yield stress.

To cope with extreme variations of the strain rate, additive viscosity is described an hyperbolic sine function of the cumulated plastic strain [2], and the (visco)plastic strain rate – derived by a generalized normality rule from a pseudo-potential – is written as

$$\dot{\underline{\underline{\varepsilon}}}^{p} = \frac{\dot{\varepsilon}_{0_{(T)}}}{\left(1-D_d\right)\left(1-D_c\right)} \left[\sinh \left\langle \frac{f_p}{K_{(T)}} \right\rangle \right]^{N} \frac{3}{2} \frac{\left(\underline{\underline{\sigma}}^{D} - \underline{\underline{X}}_1 - \underline{\underline{X}}_2\right)}{J_2\left(\underline{\underline{\sigma}} - \underline{\underline{X}}_1 - \underline{\underline{X}}_2\right)} \tag{4a}$$

$$\text{with} \quad \dot{\varepsilon}_{0(T)} = \sum_{i=1}^{3} f_i \exp\left(-\frac{Q_i}{RT}\right) \tag{4b}$$

where $K_{(T)}$, N, f, Q are material parameters and R the Boltzmann constant. A partition of the whole temperature range is de facto introduced by the three Arrhenius terms appearing in Equation (4b) in order to take account of fundamentally different viscous behaviours below $0.40T_m$ and above $0.60T_m$.

The two kinematic and isotropic hardening variables are introduced to allow the description of slow and rapid saturation mechanisms within the whole temperature range. The isotropic hardenings are chosen of the standard Voce type [3] whereas the kinematic variables are of the Armstrong & Frederick type [4], so that

$$\dot{R}_i = \dot{\varepsilon}_{0(T)} \left[\sinh \left\langle \frac{f_p}{K_{(T)}} \right\rangle \right]^N \left(a_{i_{(T)}} - b_{i_{(T)}} R_i \right) + \frac{1}{a_{i_{(T)}}} \frac{\partial a_{i_{(T)}}}{\partial T} \dot{T} R_i \quad \text{with} \quad i=1,2 \tag{5a}$$

and $$\underline{\underline{\dot{X}}}_i = \frac{2}{3} C_{i_{(T)}} \underline{\underline{\dot{\varepsilon}}}^p - D_{i_{(T)}} \underline{\underline{X}}_i \dot{p} + \frac{1}{C_{i_{(T)}}} \frac{\partial C_{i_{(T)}}}{\partial T} \dot{T} \underline{\underline{X}}_i \quad \text{with} \quad i=1,2 \tag{5b}$$

where $a_{i\,(T)}$ and $b_{i(T)}$ are material parameters, and where the cumulated plastic strain rate is computed as

$$\dot{p} = \sqrt{\frac{2}{3} \underline{\underline{\dot{\varepsilon}}}^p : \underline{\underline{\dot{\varepsilon}}}^p} \tag{6}$$

Depending on the thermo-mechanical loading, this copper alloy exhibits two different macroscopic damage mechanisms. The Lemaitre ductile damage model [5] has been chosen to represent their respective evolution laws, so that

$$\dot{D}_c = \left(\frac{\sigma^2}{2E S_{c_{(T)}} (1-D_d)(1-D_c)^2} \right)^{S_{c(T)}} \dot{p} \quad \text{as long as } D_c \le D_{ccrit_{(T)}} \tag{7a}$$

and $$\dot{D}_d = \left(\frac{\sigma^2}{2E S_{d_{(T)}} (1-D_c)(1-D_d)^2} \right)^{S_{d(T)}} \dot{p}\ H\left(\mathrm{Max}_t \left(\left\| \underline{\underline{\varepsilon}}^p \right\| \right) - \varepsilon^p_{d_{(T)}} \right) \quad \text{as long as } D_d \le D_{dcrit_{(T)}} \tag{7b}$$

where $S_{c(T)}$, $s_{c(T),}$, $S_{d(T)}$, $s_{d(T)}$, $\varepsilon^p_{d_{(T)}}$ represent material parameters and where $D_{ccrit(T)}$ and $D_{dcrit(T)}$ represent critical damage parameters.

It is assumed that local rupture occurs when $D_d \ge D_{dcrit(T)}$ or $D_c \ge D_{ccrit(T)}$.

3 Identification procedure: validity range and strategy

The model must be identified from tests that are representative of monotonous and cyclic mechanical loading up to rupture over the whole strain rate range, viz. [10^{-6} s^{-1}, 10^{-1} s^{-1}], and over the whole temperature range, viz. [$0.015T_m$, $0.81T_m$] where T_m represents the material melting temperature.

The recommended identification strategy to identify the EVP model from isothermal tension, creep and low cycle fatigue tests, is the following.

A. Firstly, at each temperature:

- Young's modulus $E_{(T)}$ is identified from low cycle fatigue and tension tests, whereas thermal expansion coefficient $\alpha_{(T;Tref)}$ is identified from a dilatometry test.

- Viscosity parameters $K_{(T)}$, N, f, Q, are identified from relaxation and fatigue relaxation tests; Figures 2-3

illustrate viscous stress evolution over the considered temperature and strain rate ranges.

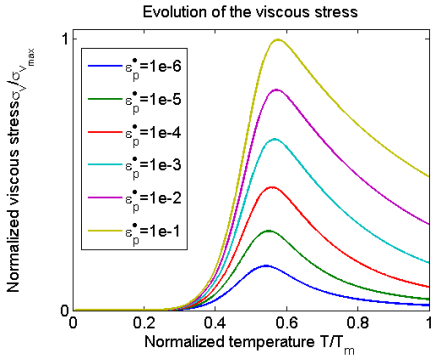

FIG. 2: Viscous stress vs. temperature

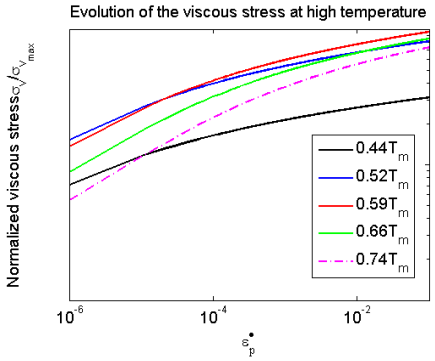

FIG. 3: Viscous stress vs. plastic strain rate

- Isotropic hardening evolutions are identified from low cycle fatigue tests; more precisely rapid and slow cyclic hardening/softening are respectively associated to the R_1 and R_2 components.

- Rapid kinematic hardening evolution – that is associated to X_1 component – is identified from low cycle fatigue tests and from the primary part of creep tests, whereas slow kinematic hardening – that is associated to X_2 component – is identified from tension tests; Figure 4 illustrates the temperature evolution of the value of kinematic hardenings at saturation.

- Initial yield strength $\sigma_{y(T)}$ is identified from both tension and low cycle fatigue tests; Figure 5 illustrates the temperature evolution of the yield stress.

B. Secondly, an optimization of the parameters set is made for all these loadings over the entire temperature range.

C. Finally, each parameter of the model is optimized so that its evolution is monotonic with temperature, a key factor of robustness of the identified model during a structural analysis.

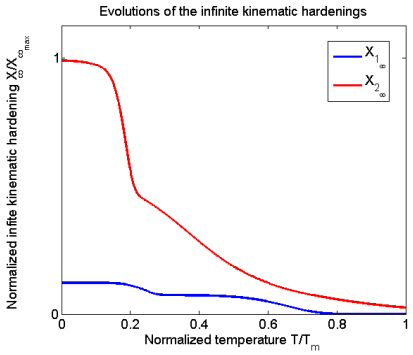

FIG. 4: Kinematic hardening at saturation vs. temperature

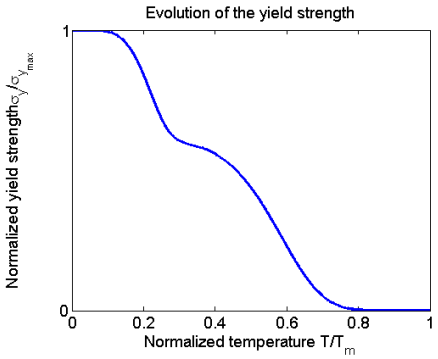

FIG. 5: Yield strength vs. temperature

The identification of damage evolutions is also made in several stages:

A. Firstly, at each temperature:

- $S_{c(T)}$, $s_{c(T)}$ parameters of D_c damage variable kinetic law are identified from the stress extrema plots of the fatigue tests, whereas the damage critical parameter $D_{ccrit(T)}$ is adjusted from the numbers of cycles to failure.

- $\varepsilon^{p}_{d(T)}$ threshold is identified from the primary part of the creep tests, whereas $S_{d(T)}$ and $s_{d(T)}$ parameters are identified from the tension tests.

- Critical damage parameter $D_{dcrit(T)}$ is adjusted from both the creep times to failure and the tension strains to failure.

B. Finally, each parameter of the damage models is optimized so that its evolution is monotonic with temperature, a key factor of robustness of the identified model during a structural analysis.

4 Results of model identification

Unfortunately the experimental data base that is available for the material considered herein is not sufficient to apply the identification procedure described above.

The tests that are available at each temperature are limited to creep tests at two different stress levels, tensile tests at three different strain rates and one $R_\varepsilon = \varepsilon_{min}/\varepsilon_{max} = 0$ fatigue test at a given strain rate.

Since relaxation or fatigue-relaxation tests results are not available, several iterations where necessary to obtain an optimal set of parameters.

Typical results for creep, monotonic tension and low cycle fatigue at $0.52T_m$ are given in Figures 6-9.

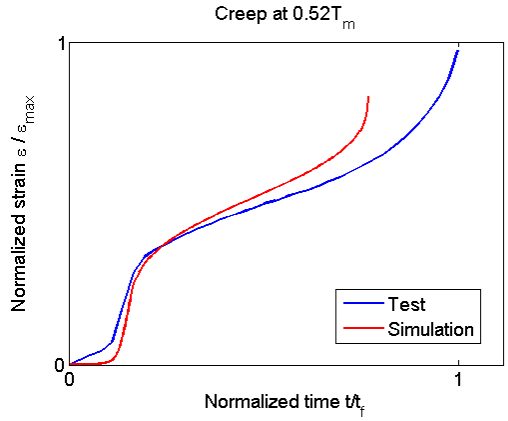

FIG. 6: Experimental result vs. model prediction for a creep test at $0.52T_m$

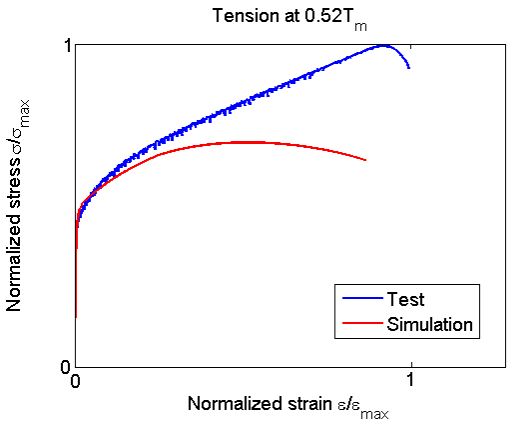

FIG. 8: Experimental result vs. model prediction for a tension test at $0.52T_m$

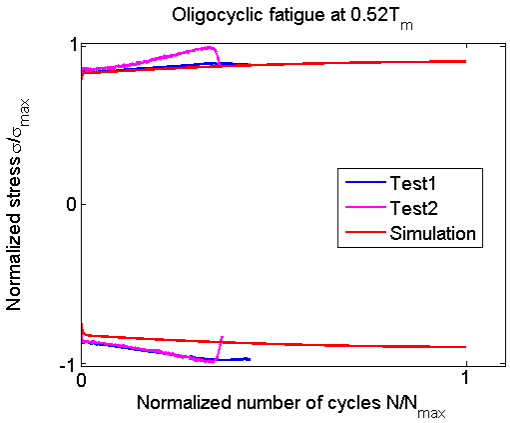

FIG. 7: Experimental result vs. model prediction for a low cycle fatigue test at $0.52T_m$

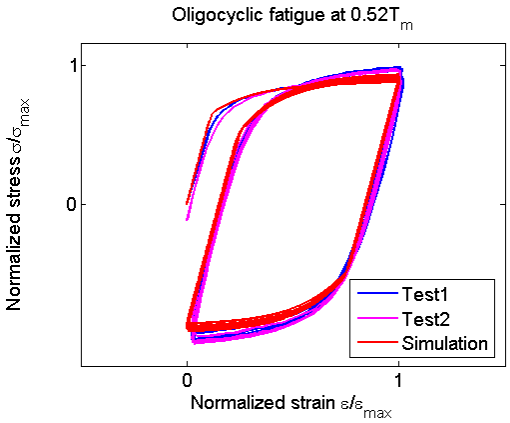

FIG. 9: Experimental result vs. model prediction for the first 5 cycles of a low cycle fatigue test at $0.52T_m$

Typical results for low cycle fatigue at $0.44T_m$ and $0.59\ T_m$ are given in Figures 10-11. It can be noticed that cyclic hardening shifts to cyclic softening at about $0.55\ T_m$.

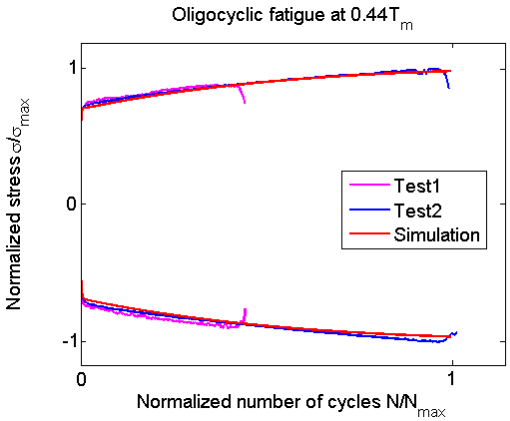

FIG. 10: Experimental result vs. model prediction for a low cycle fatigue test at $0.44T_m$ (stress extrema plot)

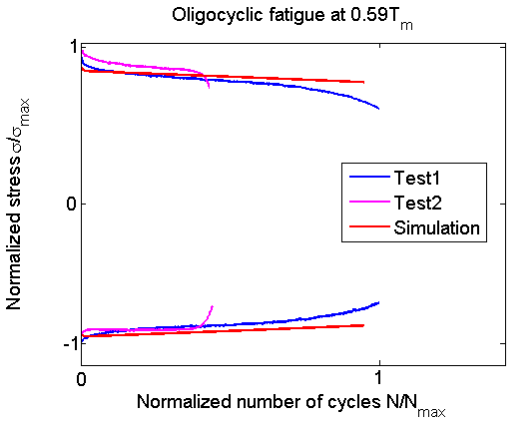

FIG. 11: Experimental result vs. model prediction for a low cycle fatigue test at $0.59T_m$ (stress extrema plot)

5 Conclusions

The study reported in this paper brings out significant improvements in the rocket engine copper alloy combustion chamber lifetime calculation methodology thanks to the use of a specific Elasto-ViscoPlasticity Damage model. This model allows to solve both the non linear damage accumulation problem and the evolution of the material properties as damage increases [6].

The non-linear and non-continuous evolution of both damage variables is clearly shown and is very much representative of the physical reality of the phenomena which occur in the combustion chamber cooling channel.

Among various possible improvements of the model, it can be noticed that according to some microscopic observations one of the damage mechanisms should be modelled by an anisotropic variable.

References:

[1] Lemaitre J., Chaboche J.L., Mécanique des matériaux solides, Ed. Dunod, 1988.
[2] Eyring H., Viscosity, plasticity, and diffusion as exemples of absolute reaction rates, Journal of Chemical Physics, 4, 283-291, 1936.
[3] Voce E., The relationship between stress and strain for homogeneous deformation, Journal Inst. Metals, 74, 537-562, 1948.
[4] Armstrong P.J., Frederick C.O., A mathematical representation of the multiaxial Baushinger effect, CEGB Report, Berkeley Nuclear Laboratories, RD/B/N731, 1966.
[5] Lemaitre J., A continuous damage mechanics model for ductile fracture, Journal of Engineering Materials and Technology, 107, 83-89, 1985.
[6] Vincent S., Petry C., Billardon R., Sagnier S., Du Tertre A., Creep-fatigue interaction with a damage coupled material behaviour law : an application for Vulcain engine, SF2M 2007 – Journées annuelles de métallurgie et de matériaux, 2007.